AUT Journal of Civil Engineering

AUT J. Civil Eng., 1(2) (2017) 145-152
DOI: 10.22060/ceej.2017.12358.5184

# Buckling Analysis of Functionally Graded Plates Based on Two-Variable Refined Plate Theory Using the Bubble Finite Strip Method

Omid Kianian, Saeid Sarrami-Foroushani*, Mojtaba Azhari

Department of Civil Engineering, Isfahan University of Technology, Isfahan, 84156-83111, Iran

**ABSTRACT:** Functionally graded materials (FGMs) have been widely used in many structural applications over the past decades. The rapid growth of the FGMs is due to their remarkable mechanical and thermal properties. The mechanical buckling analysis of functionally graded ceramic-metal rectangular plates is considered in this paper. The two-variable refined plate theory (RPT), in conjunction with the bubble finite strip method, is employed for the first time to evaluate the mechanical buckling loads of rectangular FGM plates. The theory, which has a strong similarity with the classical plate theory (CPT) in many aspects, accounts for a quadratic variation of transverse shear strains across the thickness of the plate and satisfies the zero traction boundary conditions on the top and bottom surfaces of the plate without using the shear correction factor. In comparison with the ordinary finite strip method, the convergence of the bubble finite strip method is very rapid due to using bubble shape functions. The mechanical properties of the FGM plate are assumed to vary according to a power law distribution of the volume fraction of constituents. The accuracy and efficiency of the present method are confirmed by comparing the present results with those available in the literature. Furthermore, the effects of power-law index, plate thickness, aspect ratio, loading types and various boundary conditions on the critical buckling load of the functionally graded rectangular plates are investigated.

**Review History:**

Received: 4 January 2017
Revised: 1 March 2017
Accepted: 5 August 2017
Available Online: 1 September 2017

**Keywords:**

Functionally graded plate
Refined plate theory
Buckling
Finite strip method
Bubble function

## 1- Introduction

A large number of plate theories have been developed to analyze plate structures. The classical plate theory (CPT) is the most popular theory which neglects the transverse shear deformation effects. This theory provides rational results for the thin plate [1], however, it underestimates the deflections and overestimates the natural frequencies as well as buckling loads of moderately thick and thick plates. To overcome these defects, the shear deformation plate theories such as first-order shear deformation theory (FSDT) [2-5] and higher-order shear deformation theories (HSDT) [6-11] as well as the refined plate theory (RPT) [12] are proposed. In the RPT, it is assumed that the in-plane and transverse displacements consist of bending and shear components in which the bending components do not contribute toward shear forces and, likewise, the shear components do not contribute toward bending moments. Contrary to the FSDT which needs shear correction factor, the transverse shear strains across the thickness of the plate are quadratic in the RPT. Consequently, the zero traction boundary conditions on the top and bottom surfaces of the plate is satisfied. This is the most interesting feature of the RPT, while it uses fewer unknowns. This theory is successfully developed and used to analyze functionally graded plates [13, 14].

In this study, the mechanical buckling analysis of functionally graded ceramic-metal rectangular plates is considered. The two-variable refined plate theory, in conjunction with the bubble finite strip method, is employed in the current formulation. The bubble functions are used to increase the convergence of the finite strip method.

Corresponding author, E-mail: sarrami@cc.iut.ac.ir

## 2- Mechanical properties of FG rectangular plate

Consider a rectangular functionally graded plate of total thickness h, side length a in x-direction and b in y-direction as shown in Figure 1. A coordinate system $(x, y, z)$ is established on the middle plane of the plate. The plate is made of isotropic material and the material properties are assumed to vary through the thickness according to the power law distribution [15]:

$$P(z) = (P_c - P_m)V_c + P_m \tag{1}$$

$$V_c = \left(\frac{1}{2} + \frac{z}{h}\right)^n ; (n \geq 0) \tag{2}$$

where $P_m$ and $P_c$ are the properties of the metal and ceramic, respectively. $V_c$ is the volume fraction of the ceramic and $n$ is the power law index. The Poisson's ratio, $V$, is assumed to be a constant for convenience.

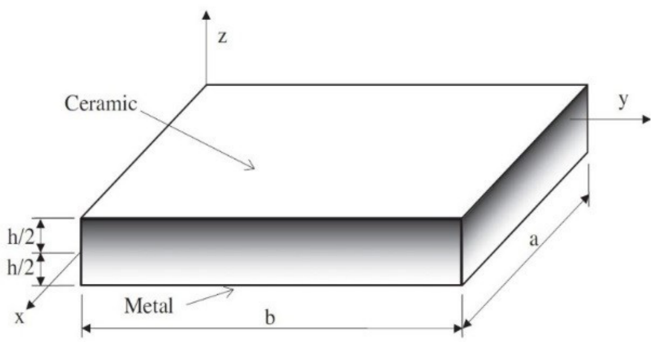


**Fig. 1. Functionally graded plate and its dimensions.**

### 3- Displacement field

Based on the assumptions of RPT [12, 16], the displacement field is defined as:

$$u(x,y,z) = -(z-z_0)\frac{\partial w_b}{\partial x} + F(z-z_0)\frac{\partial w_s}{\partial x} \tag{3}$$

$$v(x,y,z) = -(z-z_0)\frac{\partial w_b}{\partial y} + F(z-z_0)\frac{\partial w_s}{\partial y} \tag{4}$$

$$w(x,y,z) = w_b(x,y) + w_s(x,y) \tag{5}$$

where $F(z) = z\left[\frac{1}{4} - \frac{5}{3}\left(\frac{z}{h}\right)^2\right]$, and $w_b$ are $w_s$ the bending and shear components of transverse displacement, respectively and $z_0$ is the position of the neutral surface which is defined as [16]:

$$z_0 = \frac{\int_{-h/2}^{h/2} E(z) z\, dz}{\int_{-h/2}^{h/2} E(z)\, dz} \tag{6}$$

in which $E(z)$ is the modulus of elasticity of FG plate and follows the power law distribution as introduced in Equation 1.

### 4- Stability equation

After calculating the strain energy and the potential energy of the external forces, Hamilton's principle is used to derive the equations of motion appropriate to the displacement field and the constitutive equation. According to the RPT, the governing equations of the buckling analysis of FG plate can be written as [16, 17]:

$$\begin{aligned} &D_b \nabla^2\nabla^2 w_b + D_{bs}\nabla^2\nabla^2 w_s = \\ &n_x\left(\frac{\partial^2 w_b}{\partial x^2} + \frac{\partial^2 w_s}{\partial x^2}\right) + n_y\left(\frac{\partial^2 w_b}{\partial y^2} + \frac{\partial^2 w_s}{\partial y^2}\right) \end{aligned} \tag{7a}$$

$$\begin{aligned} &D_{bs}\nabla^2\nabla^2 w_b + \left(D_s\nabla^2\nabla^2 - \frac{C(1-\nu)}{2}\nabla^2\right) w_s = \\ &n_x\left(\frac{\partial^2 w_b}{\partial x^2} + \frac{\partial^2 w_s}{\partial x^2}\right) + n_y\left(\frac{\partial^2 w_b}{\partial y^2} + \frac{\partial^2 w_s}{\partial y^2}\right) \end{aligned} \tag{7b}$$

in which $D_b$, $D_{bs}$, $D_s$ and $C$ are defined as follows:

$$D_b = \int_{-h/2}^{h/2} H \times (z-z_0)\, dz \tag{8a}$$

$$D_{bs} = \int_{-h/2}^{h/2} H \times F(z) \times (z-z_0)\, dz \tag{8b}$$

$$D_s = \int_{-h/2}^{h/2} H \times F(z) \times (F(z)-d)\, dz \tag{8c}$$

$$C = \int_{-h/2}^{h/2} H \times F^2(z)\, dz \tag{8d}$$

where $H = \frac{E(z)}{1-\nu^2}$ and $d = \int_{-h/2}^{h/2} \frac{E(z)F(z)}{E(z)} dz$ .

### 5- Solution by refined finite strip method

The bubble finite strip method (BFSM) is employed here to investigate the buckling behavior of FG rectangular plates with different boundary conditions. Figure 2a shows a single strip of length bs and width as in the rectangular coordinate system ($x$, $y$, $z$) with two nodal lines of $i$ and $j$. The strip nodal degrees of freedom are shown in Figure 2b.

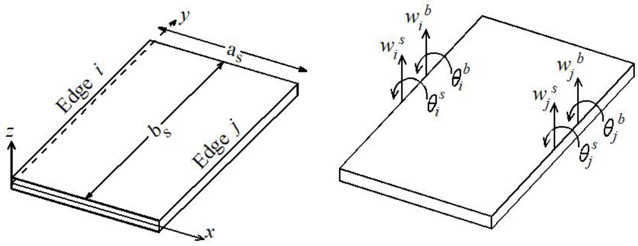


(a) (b)

**Fig. 2. a) The strip and b) Nodal degrees of freedom**

The bending and shear deflections of the strip are defined, respectively as:

$$w_b(x,y) = \sum_{q=1}^{r} \mathbf{N}_q^b \delta_q^b \tag{9a}$$

$$w_s(x,y) = \sum_{q=1}^{r} \mathbf{N}_q^s \delta_q^s \tag{9b}$$

in which $r$ is the number of harmonic modes and

$$\begin{aligned} \mathbf{N}_q^b = \mathbf{N}_q^s = [&1-3\xi^2+2\xi^3 \quad a_s(\xi-2\xi^2+\xi^3) \\ &\xi^2(\xi-1)^2 \quad 3\xi^2-2\xi^3 \quad a_s(-\xi^2+\xi^3)] Y_q(y) \end{aligned} \tag{10}$$

where $\xi = x/a_s$ and $Y_q(y)$ is the $q^{th}$ mode of a trigonometric function which are given in [17]. $Y_q(y)$ is chosen such that it satisfies the boundary conditions in one direction. $\boldsymbol{\delta}_q^b$ and $\boldsymbol{\delta}_q^s$ which are the displacement vectors related to mode $q$, are given by:

$$\delta_q^b = \left\{ w_i^b \quad \theta_i^b \quad w_{bub}^b \quad w_j^b \quad \theta_j^b \right\}_q^T \tag{11a}$$

$$\delta_q^s = \left\{ w_i^s \quad \theta_i^s \quad w_{bub}^s \quad w_j^s \quad \theta_j^s \right\}_q^T \tag{11b}$$

in which $(w_i^b)_q$, $(w_j^b)_q$, $(\theta_i^b)_q$ and $(\theta_j^b)_q$ are bending degrees of freedom of each nodal line, whereas $(w_i^s)_q$, $(w_j^s)_q$, $(\theta_i^s)_q$ and $(\theta_j^s)_q$ are the shear degrees of freedom and $\theta = \partial w/\partial x$. $(w_{bub}^b)_q$ and $(w_{bub}^s)_q$ are the degrees of freedom corresponding to the third shape function in Equation 10 which is called bubble function. These bubble displacements belong to the middle line between the two nodal lines $i$ and $j$. Assuming the bending and shear deflections of the nanoplate as expressed in Equations 9a and b, the method of weighted residuals is then applied to the Equations 7a and 7b which should be solved simultaneously. In the absence of the lateral load, the buckling equations of a plate could be written as:

$$(\mathbf{K}-\mathbf{K}_G)\delta=\mathbf{0} \tag{12}$$

in which $\boldsymbol{\delta}$ is the eigenvector; $\mathbf{K}$ is the stiffness matrix of the plate and $\mathbf{K_G}$ is the stability matrix. The stiffness matrix of a strip corresponding to $m^{th}$ and $n^{th}$ modes, $(\mathbf{K})^e_{mn}$, which is a 10×10 matrix is defined as:

$$(\mathbf{K})^{\mathrm{e}}_{\mathrm{mn}}=\begin{bmatrix} \int_0^b\int_0^a \left(\mathbf{B}^b_m\right)^T \mathbf{D}_b \left(\mathbf{B}^b_n\right)dx\,dy & \int_0^b\int_0^a \left(\mathbf{B}^b_m\right)^T \mathbf{D}_{bs} \left(\mathbf{B}^b_n\right)dx\,dy \\ \int_0^b\int_0^a \left(\mathbf{B}^b_m\right)^T \mathbf{D}_{bs} \left(\mathbf{B}^b_n\right)dx\,dy & \int_0^b\int_0^a \left(\mathbf{B}^s_m\right)^T \mathbf{D}_s \left(\mathbf{B}^s_n\right)dx\,dy \end{bmatrix} \tag{13}$$

where

$$\mathbf{B}^b_q=\begin{bmatrix} -\frac{1}{a_s^2}(-6+12\xi)Y_q & -\frac{1}{a_s}(-4+6\xi)Y_q & -\frac{1}{a_s^2}(12\xi^2-12\xi+2)Y_q & -\frac{1}{a_s^2}(6-12\xi)Y_q & -\frac{1}{a_s}(-2+6\xi)Y_q \\ -(1-3\xi^2+2\xi^3)Y_q'' & -a_s(\xi-2\xi^2+\xi^3)Y_q'' & -\xi^2(\xi-1)^2Y_q'' & -(3\xi^2-2\xi^3)Y_q'' & -a_s(-\xi^2+\xi^3)Y_q'' \\ -\frac{2}{a_s}\left(-6\xi+6\xi^2\right)Y_q' & -2\left(1-4\xi+3\xi^2\right)Y_q' & -\frac{2}{a_s}(4\xi^3+2\xi-6\xi^2)Y_q' & -\frac{2}{a_s}\left(6\xi-6\xi^2\right)Y_q' & -2\left(-2\xi+3\xi^2\right)Y_q' \end{bmatrix}_{3\times5} \tag{14}$$

$$\mathbf{B}^s_q=\begin{bmatrix} -\frac{1}{a_s^2}(-6+12\xi)Y_q & -\frac{1}{a_s}(-4+6\xi)Y_q & -\frac{1}{a_s^2}(12\xi^2-12\xi+2)Y_q & -\frac{1}{a_s^2}(6-12\xi)Y_q & -\frac{1}{a_s}(-2+6\xi)Y_q \\ -(1-3\xi^2+2\xi^3)Y_q'' & -a_s(\xi-2\xi^2+\xi^3)Y_q'' & -\xi^2(\xi-1)^2Y_q'' & -(3\xi^2-2\xi^3)Y_q'' & -a_s(-\xi^2+\xi^3)Y_q'' \\ -\frac{2}{a_s}\left(-6\xi+6\xi^2\right)Y_q' & -2\left(1-4\xi+3\xi^2\right)Y_q' & -\frac{2}{a_s}(4\xi^3+2\xi-6\xi^2)Y_q' & -\frac{2}{a_s}\left(6\xi-6\xi^2\right)Y_q' & -2\left(-2\xi+3\xi^2\right)Y_q' \\ -\left(1-3\xi^2+2\xi^3\right)Y_q' & -a_s(\xi-2\xi^2+\xi^3)Y_q' & -\xi^2(\xi-1)^2Y_q' & -(3\xi^2-2\xi^3)Y_q' & -a_s(-\xi^2+\xi^3)Y_q' \\ -\frac{1}{a_s}\left(-6\xi+6\xi^2\right)Y_q & -\left(1-4\xi+3\xi^2\right)Y_q & -\frac{1}{a_s}(4\xi^3+2\xi-6\xi^2)Y_q & -\frac{1}{a_s}\left(6\xi-6\xi^2\right)Y_q & -\left(-2\xi+3\xi^2\right)Y_q \end{bmatrix}_{5\times5} \tag{15}$$

In these equations, $Y'_q$ and $Y''_q$ represent the first and second derivatives of $Y_q$ with respect to y, respectively; also

$$\mathbf{D}_b=D_b\begin{bmatrix} 1 & \nu & 0 \\ \nu & 1 & 0 \\ 0 & 0 & \frac{1-\nu}{2} \end{bmatrix},\mathbf{D}_{bs}=D_{bs}\begin{bmatrix} 1 & \nu & 0 \\ \nu & 1 & 0 \\ 0 & 0 & \frac{1-\nu}{2} \end{bmatrix} \tag{16}$$

and

$$\mathbf{D}_s=\begin{bmatrix} D_s & \nu D_s & 0 & 0 & 0 \\ \nu D_s & D_s & 0 & 0 & 0 \\ 0 & 0 & \frac{(1-\nu)D_s}{2} & 0 & 0 \\ 0 & 0 & 0 & \frac{(1-\nu)C}{2} & 0 \\ 0 & 0 & 0 & 0 & \frac{(1-\nu)C}{2} \end{bmatrix} \tag{17}$$

$(\boldsymbol{K}_G^L)^e_{mn}$ is also defined as:

$$\left(\mathbf{K}_G^L\right)^e_{mn}=\begin{bmatrix} \int_0^b\int_0^a \mathbf{B}^{\mathrm{T}}_{\mathrm{Gm}}\mathbf{S}_L\mathbf{B}_{\mathrm{Gn}}\,dx\,dy & \int_0^b\int_0^a \mathbf{B}^{\mathrm{T}}_{\mathrm{Gm}}\mathbf{S}_L\mathbf{B}_{\mathrm{Gn}}\,dx\,dy \\ \int_0^b\int_0^a \mathbf{B}^{\mathrm{T}}_{\mathrm{Gm}}\mathbf{S}_L\mathbf{B}_{\mathrm{Gn}}\,dx\,dy & \int_0^b\int_0^a \mathbf{B}^{\mathrm{T}}_{\mathrm{Gm}}\mathbf{S}_L\mathbf{B}_{\mathrm{Gn}}\,dx\,dy \end{bmatrix}_{10\times10} \tag{18}$$

where

$$\mathbf{B}^T_{Gq}=\begin{bmatrix} \frac{1}{a_s}(-6\xi+6\xi^2)Y_q & (1\text{-}3\xi^2+2\xi^3)Y_q' \\ (1-4\xi+3\xi^2)Y_q & a_s(\xi-2\xi^2+\xi^3)Y_q' \\ \frac{1}{a_s}(4\xi^3+2\xi-6\xi^2)Y_q & \xi^2(\xi-1)^2Y_q' \\ \frac{1}{a_s}(6\xi-6\xi^2)Y_q & (3\xi^2\text{-}2\xi^3)Y_q' \\ (-2\xi+3\xi^2)Y_q & a_s(-\xi^2+\xi^3)Y_q' \end{bmatrix} \tag{19}$$

and

$$\mathbf{S}_L=\begin{bmatrix} N_{xx} & 0 \\ 0 & N_{yy} \end{bmatrix} \tag{20}$$

It should be noted that $N_{xx}=\sigma_x h$ and $N_{yy}=\sigma_y h$. $\sigma_x$ and $\sigma_y$ are stresses parallel to x-direction and y-direction, respectively. Having the finite strip formulation, a computer program is developed in the MATLAB environment to study the buckling of FGM plates. To obtain the total stiffness and stability matrices in Equation 12, the plate is first divided into a proper number of strips. Then, the stiffness and stability matrices of each strip are computed using Equations 13 and 18. The matrices are finally assembled using the equilibrium and compatibility equations along the nodal lines. The boundary conditions are then applied and finally the eigenvalue problem in Equation 12 is solved by vanishing the determinant of the coefficient matrix as:

$$\left|\mathbf{K}-\mathbf{K}_G\right|=0 \tag{21}$$

Equation 21 is solved to obtain the critical buckling stress of the FGM plate.

## 6- Results and discussion

In order to validate the accuracy and efficiency of the present formulation, several examples are presented and discussed. Table 1 shows the material properties of the FG plate.

**Table 1. Material properties**

| Material | $E_m$ | $E_c$ | $\nu$ |
|---|---|---|---|
| Al / $Al_2O_3$ | 70 GPa | 380 GPa | 0.3 |

The comparison of non-dimensional critical buckling load, $N=N_{cr}a^2/E_m h^3$, for a simply supported FG plate subjected to uniaxial compression along the *x*-axis, biaxial compression and biaxial compression (along *x*-axis) and tension (along *y*-axis) are presented in Table 2-4, respectively. Different width to thickness ratios, *a/h*, aspect ratios, *b/a*, and power law index, *n*, are considered in the results. It can be seen that the non-dimensional critical buckling loads obtained based on the present study are in an excellent agreement with those reported by Thai and Choi [18].

Table 5 shows non-dimensional buckling load, *N*, for square FG plate under uniaxial compression with different boundary conditions and several widths to thickness ratios, *a/h*. Different values of power law index, *n*, are also taken. In Table 5, S, C, F, and G simply refer to clamped, free and guided supports, respectively.

All the results presented in Tables 2-5 indicate that the proposed BFSM is a powerful method to solve the buckling of FGM plates with any boundary conditions and different

**Table 2. Non-dimensional critical buckling load of simply supported FG plate under uniaxial compression along the x-axis**

| *a/b* | *a/h* | Method | *n* | | | | | | | | |
|---|---|---|---|---|---|---|---|---|---|---|---|
| | | | 0 | 0.5 | 1 | 2 | 5 | 10 | 20 | 100 | inf |
| 0.5 | 5 | RPT[18] | 6.7203 | 4.4235 | 3.4164 | 2.6451 | 2.1484 | 1.9213 | 1.7115 | 1.3737 | --- |
| | | Present | 6.7204 | 4.4235 | 3.4164 | 2.6451 | 2.1484 | 1.9213 | 1.7115 | 1.3737 | 1.2379 |
| | 10 | RPT[18] | 7.4053 | 4.8206 | 3.7111 | 2.8897 | 2.4165 | 2.1896 | 1.9387 | 1.5251 | --- |
| | | Present | 7.4054 | 4.8207 | 3.7111 | 2.8897 | 2.4165 | 2.1896 | 1.9387 | 1.5250 | 1.3641 |
| | 20 | RPT[18] | 7.5993 | 4.9315 | 3.793 | 2.9582 | 2.4944 | 2.269 | 2.0054 | 1.5683 | --- |
| | | Present | 7.5994 | 4.9315 | 3.7931 | 2.9582 | 2.4944 | 2.2690 | 2.0054 | 1.5683 | 1.3998 |
| | 50 | RPT[18] | 7.6555 | 4.9634 | 3.8166 | 2.9779 | 2.5172 | 2.2923 | 2.025 | 1.5809 | --- |
| | | Present | 7.6556 | 4.9635 | 3.8167 | 2.9779 | 2.5172 | 2.2923 | 2.0250 | 1.5809 | 1.4102 |
| | 100 | RPT[18] | 7.6635 | 4.968 | 3.82 | 2.9808 | 2.5205 | 2.2957 | 2.0278 | 1.5827 | --- |
| | | Present | 7.6637 | 4.9681 | 3.8201 | 2.9808 | 2.5205 | 2.2957 | 2.0278 | 1.5827 | 1.4117 |
| 1 | 5 | RPT[18] | 16.0211 | 10.6254 | 8.2245 | 6.3432 | 5.0531 | 4.4807 | 4.007 | 3.2586 | --- |
| | | Present | 16.0211 | 10.6254 | 8.2245 | 6.3432 | 5.0531 | 4.4807 | 4.0070 | 3.2586 | 2.9512 |
| | 10 | RPT[18] | 18.5785 | 12.1229 | 9.3391 | 7.2631 | 6.0353 | 5.4528 | 4.8346 | 3.8198 | --- |
| | | Present | 18.5786 | 12.1230 | 9.3391 | 7.2631 | 6.0353 | 5.4528 | 4.8346 | 3.8198 | 3.4223 |
| | 20 | RPT[18] | 19.3528 | 12.5668 | 9.6675 | 7.5371 | 6.3448 | 5.7668 | 5.0988 | 3.9923 | --- |
| | | Present | 19.3529 | 12.5668 | 9.6675 | 7.5371 | 6.3448 | 5.7668 | 5.0988 | 3.9923 | 3.5650 |
| | 50 | RPT[18] | 19.5814 | 12.697 | 9.7636 | 7.6177 | 6.4373 | 5.8614 | 5.1782 | 4.0434 | --- |
| | | Present | 19.5815 | 12.6971 | 9.7637 | 7.6177 | 6.4373 | 5.8614 | 5.1781 | 4.0434 | 3.6071 |
| | 100 | RPT[18] | 19.6145 | 12.7158 | 9.7775 | 7.6293 | 6.4507 | 5.8752 | 5.1897 | 4.0508 | --- |
| | | Present | 19.6146 | 12.7159 | 9.7776 | 7.6293 | 6.4507 | 5.8752 | 5.1897 | 4.0508 | 3.6132 |
| 1.5 | 5 | RPT[18] | 28.1996 | 19.251 | 15.0344 | 11.4234 | 8.4727 | 7.2952 | 6.6106 | 5.6325 | --- |
| | | Present | 28.2030 | 19.2535 | 15.0363 | 11.4248 | 8.4736 | 7.2960 | 6.6112 | 5.6331 | 5.1952 |
| | 10 | RPT[18] | 40.7476 | 26.9091 | 20.8024 | 16.0793 | 12.9501 | 11.5379 | 10.2958 | 8.3112 | --- |
| | | Present | 40.7548 | 26.9139 | 20.8062 | 16.0821 | 12.9522 | 11.5398 | 10.2975 | 8.3126 | 7.5074 |
| | 20 | RPT[18] | 45.893 | 29.905 | 23.0286 | 17.9221 | 14.9472 | 13.5273 | 11.9843 | 9.4447 | --- |
| | | Present | 45.9021 | 29.9109 | 23.0332 | 17.9257 | 14.9501 | 13.5299 | 11.9867 | 9.4466 | 8.4556 |
| | 50 | RPT[18] | 47.5786 | 30.8691 | 23.7414 | 18.5177 | 15.6238 | 14.2156 | 12.5629 | 9.8207 | --- |
| | | Present | 47.5885 | 30.8754 | 23.7463 | 18.5215 | 15.6270 | 14.2185 | 12.5654 | 9.8227 | 8.7663 |
| | 100 | RPT[18] | 47.8297 | 31.0119 | 23.8469 | 18.6061 | 15.7256 | 14.3198 | 12.6502 | 9.8769 | --- |
| | | Present | 47.8397 | 31.0184 | 23.8518 | 18.6100 | 15.7288 | 14.3228 | 12.6528 | 9.8789 | 8.8125 |

loading types. In comparison with the FEM, fewer degrees of freedom is required in the FSM. Moreover, using the bubble functions leads the method to utilize even fewer degrees of freedom than the ordinary FSM. It can be observed from the results that compared to other solution methods proposed in the literature, the BFSM is a more powerful, simple, economical and efficient method to solve the buckling problem of FG

Figure 3 indicates the effects of aspect ratio, b/a, on non-dimensional critical buckling load of simply supported FG plate subjected to uniaxial compression along *y*-axis. It can be observed that by increasing the aspect ratio, the non-dimensional buckling load decreases.

The effects of power-law index, n, on the buckling load of a simply supported square plate ($a$=$b$=10$h$) under various loading conditions are shown in Figure 4. Three loading conditions are uniaxial compression, biaxial compression (C & C), and biaxial tension and compression (T & C). It can be seen that the non-dimensional buckling load increases by

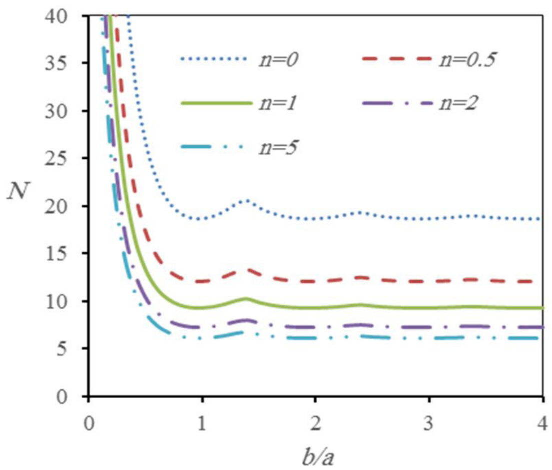


**Fig. 3. Effects of aspect ratio, b/a, on the non-dimensional critical buckling load of simply supported FG plate subjected to uniaxial compression along y-axis.**

**Table 3. Non-dimensional critical buckling load of simply supported FG plate under biaxial compression**

| *a/b* | *a/h* | Method | *n* | | | | | | | | |
|---|---|---|---|---|---|---|---|---|---|---|---|
| | | | 0 | 0.5 | 1 | 2 | 5 | 10 | 20 | 100 | inf |
| 0.5 | 5 | RPT[18] | 5.3762 | 3.5388 | 2.7331 | 2.1161 | 1.7187 | 1.537 | 1.3692 | 1.099 | --- |
| | | Present | 5.3763 | 3.5388 | 2.7331 | 2.1161 | 1.7187 | 1.5370 | 1.3692 | 1.0989 | 0.9903 |
| | 10 | RPT[18] | 5.9243 | 3.8565 | 2.9689 | 2.3117 | 1.9332 | 1.7517 | 1.551 | 1.22 | --- |
| | | Present | 5.9243 | 3.8565 | 2.9689 | 2.3117 | 1.9332 | 1.7517 | 1.5510 | 1.2200 | 1.0913 |
| | 20 | RPT[18] | 6.0794 | 3.9452 | 3.0344 | 2.3665 | 1.9955 | 1.8152 | 1.6044 | 1.2547 | --- |
| | | Present | 6.0795 | 3.9452 | 3.0344 | 2.3665 | 1.9955 | 1.8152 | 1.6043 | 1.2546 | 1.1199 |
| | 50 | RPT[18] | 6.1244 | 3.9708 | 3.0533 | 2.3823 | 2.0137 | 1.8338 | 1.62 | 1.2647 | --- |
| | | Present | 6.1244 | 3.9708 | 3.0533 | 2.3823 | 2.0137 | 1.8338 | 1.6200 | 1.2647 | 1.1281 |
| | 100 | RPT[18] | 6.1308 | 3.9744 | 3.056 | 2.3846 | 2.0164 | 1.8365 | 1.6222 | 1.2662 | --- |
| | | Present | 6.1309 | 3.9745 | 3.0560 | 2.3846 | 2.0164 | 1.8365 | 1.6222 | 1.2662 | 1.1293 |
| 1 | 5 | RPT[18] | 8.0105 | 5.3127 | 4.1122 | 3.1716 | 2.5265 | 2.2403 | 2.0035 | 1.6293 | --- |
| | | Present | 8.0105 | 5.3127 | 4.1122 | 3.1716 | 2.5265 | 2.2403 | 2.0035 | 1.6293 | 1.4756 |
| | 10 | RPT[18] | 9.2893 | 6.0615 | 4.6696 | 3.6315 | 3.0177 | 2.7264 | 2.4173 | 1.9099 | --- |
| | | Present | 9.2893 | 6.0615 | 4.6695 | 3.6315 | 3.0176 | 2.7264 | 2.4173 | 1.9099 | 1.7111 |
| | 20 | RPT[18] | 9.6764 | 6.2834 | 4.8337 | 3.7686 | 3.1724 | 2.8834 | 2.5494 | 1.9961 | --- |
| | | Present | 9.6764 | 6.2834 | 4.8337 | 3.7685 | 3.1724 | 2.8834 | 2.5494 | 1.9961 | 1.7825 |
| | 50 | RPT[18] | 9.7907 | 6.3485 | 4.8818 | 3.8088 | 3.2186 | 2.9307 | 2.5891 | 2.0217 | --- |
| | | Present | 9.7907 | 6.3485 | 4.8818 | 3.8088 | 3.2186 | 2.9307 | 2.5890 | 2.0217 | 1.8035 |
| | 100 | RPT[18] | 9.8073 | 6.3579 | 4.8888 | 3.8147 | 3.2254 | 2.9376 | 2.5948 | 2.0254 | --- |
| | | Present | 9.8073 | 6.3579 | 4.8888 | 3.8146 | 3.2253 | 2.9376 | 2.5948 | 2.0254 | 1.8066 |
| 1.5 | 5 | RPT[18] | 11.682 | 7.8299 | 6.0799 | 4.6637 | 3.6176 | 3.1718 | 2.841 | 2.36 | --- |
| | | Present | 11.682 | 7.8298 | 6.0799 | 4.6637 | 3.6175 | 3.1718 | 2.8510 | 2.3599 | 2.1519 |
| | 10 | RPT[18] | 14.6084 | 9.5685 | 7.3793 | 5.7279 | 4.7124 | 4.2384 | 3.7657 | 2.9959 | --- |
| | | Present | 14.6084 | 9.5685 | 7.3793 | 5.7278 | 4.7124 | 4.2384 | 3.7657 | 2.9959 | 2.6910 |
| | 20 | RPT[18] | 15.5887 | 10.1332 | 7.7977 | 6.0761 | 5.1006 | 4.63 | 4.0961 | 3.2135 | --- |
| | | Present | 15.5887 | 10.1332 | 7.7976 | 6.0761 | 5.1006 | 4.6299 | 4.0961 | 3.2134 | 2.8716 |
| | 50 | RPT[18] | 15.8876 | 10.3036 | 7.9236 | 6.1815 | 5.2212 | 4.7531 | 4.1995 | 3.2803 | --- |
| | | Present | 15.8876 | 10.3036 | 7.9236 | 6.1815 | 5.2212 | 4.7531 | 4.1994 | 3.2802 | 2.9266 |
| | 100 | RPT[18] | 15.9312 | 10.3284 | 7.9419 | 6.1969 | 5.2389 | 4.7712 | 4.2147 | 3.29 | --- |
| | | Present | 15.9312 | 10.3284 | 7.9419 | 6.1968 | 5.2389 | 4.7712 | 4.2146 | 3.2900 | 2.9347 |

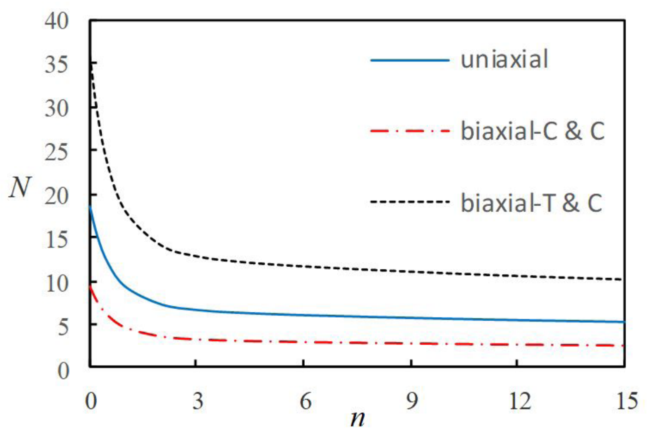


**Fig. 4. The effect of power-law index, *n*, on the buckling load of simply supported square plate (*a*=*b*=10*h*) under various loading conditions.**

decreasing the power law index under any type of loading. The convergence of the bubble finite strip method (BFSM) in comparison with the ordinary finite strip method (OFSM) is shown in Figure 5. BFSM converges very rapidly due to using the bubble functions. It can be seen that the results obtained from the BFSM with two strips are equal to those obtained from the OFSM using six strips. Therefore, it could be concluded that the degrees of freedom remarkably reduces due to using the bubble functions.

Figure 6 indicates the output sample of the developed computer program in the MATLAB environment for FG plate analysis in an especial case that $a/h = 5$, power low index, $n = 0$, and the number of strips equals to 3. The plate is square and simply supported.

**Table 4. Non-dimensional critical buckling load of simply supported FG plate under biaxial compression (along x-axis) and tension (along y-axis)**

| *a/b* | *a/h* | Method | *n* | | | | | | | | |
|---|---|---|---|---|---|---|---|---|---|---|---|
| | | | 0 | 0.5 | 1 | 2 | 5 | 10 | 20 | 100 | inf |
| 0.5 | 5 | RPT[18] | 8.9604 | 5.898 | 4.5551 | 3.5268 | 2.8646 | 2.5617 | 2.282 | 1.8316 | --- |
| | | Present | 8.9605 | 5.8981 | 4.5552 | 3.5268 | 2.8646 | 2.5617 | 2.2820 | 1.8316 | 1.6506 |
| | 10 | RPT[18] | 9.8738 | 6.4275 | 4.9481 | 3.8529 | 3.2219 | 2.9195 | 2.585 | 2.0334 | --- |
| | | Present | 9.8739 | 6.4276 | 4.9482 | 3.8529 | 3.2220 | 2.9195 | 2.5850 | 2.0334 | 1.8188 |
| | 20 | RPT[18] | 10.132 | 6.5753 | 5.0574 | 3.9442 | 3.3259 | 3.0253 | 2.6739 | 2.0911 | --- |
| | | Present | 10.132 | 6.5754 | 5.0574 | 3.9442 | 3.3259 | 3.0253 | 2.6739 | 2.0911 | 1.8665 |
| | 50 | RPT[18] | 10.207 | 6.6179 | 5.0888 | 3.9706 | 3.3562 | 3.0564 | 2.7 | 2.1079 | --- |
| | | Present | 10.207 | 6.6180 | 5.0889 | 3.9706 | 3.3563 | 3.0564 | 2.7000 | 2.1079 | 1.8803 |
| | 100 | RPT[18] | 10.218 | 6.6241 | 5.0934 | 3.9744 | 3.3606 | 3.0609 | 2.7037 | 2.1103 | --- |
| | | Present | 10.218 | 6.6241 | 5.0934 | 3.9744 | 3.3606 | 3.0609 | 2.7037 | 2.1103 | 1.8823 |
| 1 | 5 | RPT[18] | 26.2058 | 17.7704 | 13.8486 | 10.5589 | 7.959 | 6.897 | 6.232 | 5.2556 | --- |
| | | Present | 26.2111 | 17.7742 | 13.8516 | 10.5611 | 7.9605 | 6.8982 | 6.2332 | 5.2566 | 4.8283 |
| | 10 | RPT[18] | 35.8416 | 23.592 | 18.2206 | 14.1073 | 11.4583 | 10.2468 | 9.1281 | 7.3263 | --- |
| | | Present | 35.8518 | 23.5988 | 18.2258 | 14.1113 | 11.4614 | 10.2496 | 9.1306 | 7.3284 | 6.6042 |
| | 20 | RPT[18] | 39.4951 | 25.71 | 19.7925 | 15.4115 | 12.8878 | 11.6779 | 10.34 | 8.1336 | --- |
| | | Present | 39.5074 | 25.7181 | 19.7987 | 15.4163 | 12.8917 | 11.6814 | 10.3431 | 8.1361 | 7.2776 |
| | 50 | RPT[18] | 40.6574 | 26.374 | 20.2833 | 15.8219 | 13.3554 | 12.1543 | 10.7401 | 8.3931 | --- |
| | | Present | 40.6705 | 26.3825 | 20.2898 | 15.8269 | 13.3596 | 12.1581 | 10.7435 | 8.3957 | 7.4919 |
| | 100 | RPT[18] | 40.8291 | 26.4717 | 20.3554 | 15.8823 | 13.425 | 12.2256 | 10.7998 | 8.4315 | --- |
| | | Present | 40.8423 | 26.4802 | 20.3620 | 15.8874 | 13.4293 | 12.2295 | 10.8033 | 8.4342 | 7.5235 |
| 1.5 | 5 | RPT[18] | 29.0249 | 20.1105 | 15.7823 | 11.9009 | 8.525 | 7.2422 | 6.6008 | 5.7477 | --- |
| | | Present | 30.3731 | 20.3576 | 15.8078 | 12.1256 | 9.4057 | 8.24681 | 7.4127 | 6.1359 | 5.5950 |
| | 10 | RPT[18] | 37.9819 | 24.8781 | 19.1863 | 14.8925 | 12.2523 | 11.0199 | 9.7909 | 7.7894 | --- |
| | | Present | 37.9820 | 24.8782 | 19.1863 | 14.8925 | 12.2523 | 11.0198 | 9.7909 | 7.7894 | 6.9966 |
| | 20 | RPT[18] | 40.5307 | 26.3463 | 20.274 | 15.798 | 13.2616 | 12.0379 | 10.65 | 8.3551 | --- |
| | | Present | 40.5308 | 26.3463 | 20.2740 | 15.798 | 13.2616 | 12.0379 | 10.6500 | 8.3550 | 7.4662 |
| | 50 | RPT[18] | 41.3076 | 26.7894 | 20.6013 | 16.0719 | 13.5752 | 12.358 | 10.9186 | 8.5287 | --- |
| | | Present | 41.3077 | 26.7894 | 20.6013 | 16.0719 | 13.5752 | 12.3580 | 10.9186 | 8.5287 | 7.6093 |
| | 100 | RPT[18] | 41.4211 | 26.8539 | 20.6489 | 16.1118 | 13.6212 | 12.4052 | 10.9581 | 8.5541 | --- |
| | | Present | 41.4212 | 26.8539 | 20.6490 | 16.1118 | 13.6212 | 12.4052 | 10.9581 | 8.5541 | 7.6302 |

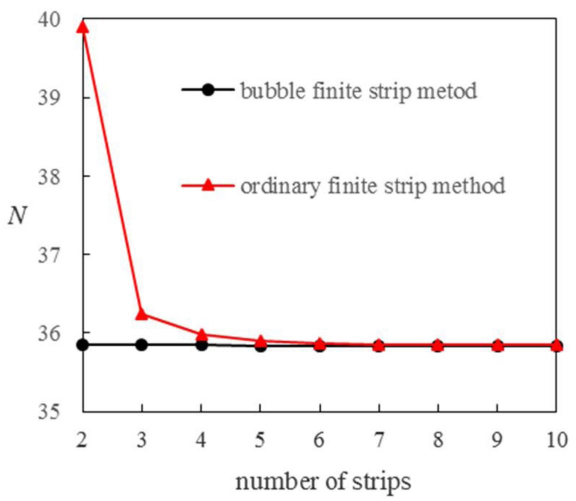


**Fig. 5. Convergence rate of BFSM in comparison with OFSM.**

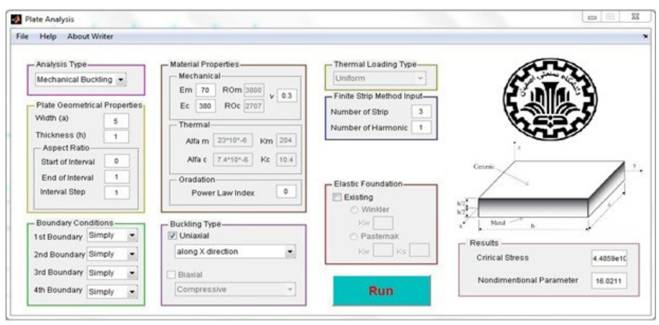


**Fig. 6. Output sample of computer program for FG plate analysis**

**Table 5. Non-dimensional uniaxial buckling load of square FG plate with different boundary conditions and width to thickness ratios, *a/h*, and various power-law index, n.**

| *a/h* | *n* | Boundary Conditions | | | | | | | | | |
|---|---|---|---|---|---|---|---|---|---|---|---|
| | | SSSS | SCSC | SSSC | SCSG | SCSF | CCCC | CCCS | CFCF | SFSF | CGCG |
| 5 | 0 | 16.0211 | 22.2749 | 17.9172 | 18.7989 | 9.7060 | 28.3686 | 24.8541 | 13.9770 | 8.6839 | 23.4881 |
| | 0.5 | 10.6254 | 15.0734 | 11.9885 | 12.6381 | 6.4308 | 19.6424 | 16.9902 | 9.3700 | 5.7252 | 16.0147 |
| | 1 | 8.2245 | 11.7394 | 9.3042 | 9.8219 | 4.9762 | 15.4114 | 13.2733 | 7.2763 | 4.4237 | 12.5019 |
| | 5 | 5.0531 | 6.78362 | 5.5617 | 5.7867 | 3.0661 | 8.3398 | 7.4445 | 4.3265 | 2.7675 | 7.0710 |
| 10 | 0 | 18.5786 | 29.6189 | 22.0175 | 23.7899 | 11.1606 | 43.4076 | 35.7661 | 17.4838 | 9.6567 | 33.5882 |
| | 0.5 | 12.1230 | 19.4544 | 14.4051 | 15.5811 | 7.2789 | 28.6964 | 23.5875 | 11.4514 | 6.2883 | 22.1671 |
| | 1 | 9.3391 | 15.0156 | 11.1057 | 12.0159 | 5.6066 | 22.1907 | 18.2270 | 8.8313 | 4.8414 | 17.1333 |
| | 5 | 6.0353 | 9.5051 | 7.1170 | 7.6739 | 3.6288 | 13.7633 | 11.3912 | 5.6403 | 3.1490 | 10.6869 |
| 20 | 0 | 19.3529 | 32.1606 | 23.3183 | 25.3402 | 11.5878 | 49.0863 | 39.8323 | 18.6505 | 9.9296 | 37.6682 |
| | 0.5 | 12.5668 | 20.9209 | 15.1524 | 16.4695 | 7.5234 | 31.9868 | 25.9391 | 12.1232 | 6.4442 | 24.5406 |
| | 1 | 9.6675 | 16.1024 | 11.6589 | 12.6730 | 5.7874 | 24.6319 | 19.9710 | 9.3290 | 4.9566 | 18.8966 |
| | 5 | 6.3448 | 10.5082 | 7.6346 | 8.2935 | 3.8001 | 15.9858 | 12.9884 | 6.1026 | 3.2588 | 12.2729 |
| 50 | 0 | 19.5815 | 32.9443 | 23.7082 | 25.7960 | 11.7127 | 50.8880 | 41.1029 | 19.0054 | 10.0084 | 38.9972 |
| | 0.5 | 12.6971 | 21.3680 | 15.3747 | 16.7290 | 7.5946 | 33.0159 | 26.6644 | 12.3255 | 6.4890 | 25.3005 |
| | 1 | 9.7637 | 16.4328 | 11.8231 | 12.8647 | 5.8400 | 25.3925 | 20.5069 | 9.4784 | 4.9898 | 19.4584 |
| | 5 | 6.4373 | 10.8242 | 7.7922 | 8.4780 | 3.8506 | 16.7107 | 13.5003 | 6.2459 | 3.2907 | 12.8066 |

## 7- Conclusion

In this study, the two-variable refined plate theory, in conjunction with the bubble finite strip method is employed for the first time to study the buckling of functionally graded rectangular plates. To decouple governing equations, the equations are written based on neutral surface. In comparison with other shear deformation plate theories, the two-variable refined plate theory uses a lower number of unknowns and therefore decreases the degrees of freedom of the system. Moreover, using the bubble functions in the interpolation of the displacement field increases the efficiency and convergence of the finite strip method. In conclusion, the proposed method is a simple, efficient, accurate and economical method to analyze the buckling of FG rectangular plates.

## References


[1] H.T. Thai, S.E. Kim, A review of theories for the modeling and analysis of functionally graded plates and shells, *Composite Structures*, 128 (2015) 70-86.

[2] E. Reissner, The effect of transverse shear deformation on the bending of elastic plates, *J. appl. Mech.*, (1945) 69-77.

[3] R.D. Mindlin, Influence of rotatory inertia and shear on flexural motions of isotropic, elastic plates, *J. appl. Mech.*, 18 (1951) 31-38.

[4] B. Shariat, M. Eslami, Buckling of functionally graded plates under in plane compressive loading based on the first order plate theory, in: *Proceeding of the Fifth International Conference on Composite Science and Technology*. Sharjah, UAE, 2005.

[5] M. Mohammadi, A. Saidi, E. Jomehzadeh, A novel analytical approach for the buckling analysis of moderately thick functionally graded rectangular plates with two simply-supported opposite edges, Proceedings of the Institution of Mechanical Engineers, Part C: *Journal of Mechanical Engineering Science*, 224(9) (2010) 1831-1841.

[6] J. Reddy, D. Robbins, Theories and computational models for composite laminates, *Applied mechanics reviews*, 47(6) (1994) 147-169.

[7] B.S. Shariat, M. Eslami, Buckling of thick functionally graded plates under mechanical and thermal loads, *Composite Structures*, 78(3) (2007) 433-439.

[8] M. Najafizadeh, H. Heydari, Higher-Order Theory For Bucklng of Functionally Graded Circular Plates, *AIAA journal*, 45(6) (2007) 1153-1160.

[9] M. Bodaghi, A. Saidi, Levy-type solution for buckling analysis of thick functionally graded rectangular plates based on the higher-order shear deformation plate theory, *Applied Mathematical Modelling*, 34(11) (2010) 3659-3673.

[10] M. Najafizadeh, H. Heydari, An exact solution for buckling of functionally graded circular plates based on higher order shear deformation plate theory under uniform radial compression, *International Journal of Mechanical Sciences*, 50(3) (2008) 603-612.

[11] T. Kant, A critical review and some results of recently developed refined theories of fiber-reinforced laminated composites and sandwiches, *Composite Structures*, 23(4) (1993) 293-312.

[12] R.P. Shimpi, Refined plate theory and its variants, *AIAA journal*, 40(1) (2002) 137-146.

[13] M.S. Ahmed Houari, S. Benyoucef, I. Mechab, A. Tounsi, E.A. Adda Bedia, Two-variable refined plate theory for thermoelastic bending analysis of functionally graded sandwich plates, *Journal of Thermal Stresses*, 34(4) (2011) 315-334.

[14] S. Mirzaei, M. Azhari, H.A.R. Bondarabady, On the use of finite strip method for buckling analysis of moderately thick plate by refined plate theory and using new types of functions, *Latin American Journal of Solids and Structures*, 12(3) (2015) 561-582.

[15] K. Swaminathan, D. Sangeetha, Thermal analysis of FGM plates–A critical review of various modeling techniques and solution methods, *Composite Structures*, 160 (2017) 43-60.

[16] D.-G. Zhang, Y.-H. Zhou, A theoretical analysis of FGM thin plates based on physical neutral surface, *Computational Materials Science*, 44(2) (2008) 716-720.

[17] S. Sarrami-Foroushani, M. Azhari, Nonlocal buckling and vibration analysis of thick rectangular nanoplates using finite strip method based on refined plate theory, *Acta Mechanica*, 227(3) (2016) 721-742.

[18] H.-T. Thai, D.-H. Choi, An efficient and simple refined theory for buckling analysis of functionally graded plates, *Applied Mathematical Modelling*, 36(3) (2012) 1008-1022.

Please cite this article using:

Omid Kianian, Saeid Sarrami-Foroushani, Mojtaba Azhari, Buckling Analysis of Functionally Graded Plates Based on Two-Variable Refined Plate Theory Using the Bubble Finite Strip Method, *AUT J. Civil Eng.*, 1(2) (2017) 145-152.

DOI: 10.22060/ceej.2017.12358.5184